Introduction into defect studies in ceramic materials(II)

Structure, Defects and Physical Properties

Z. Wang

January 18, 2002

Ceramic Crystal Structures

The majority of ceramic crystal structures are based on either FCC or HCP close-packing of one type of ion, with the other ion(s) occupying a specific set of interstitial sites. We will discuss some of the most important structures, beginning with those based on FCC anion close-packing with (1) the cations occupying octahedral sites. Then, (2)structure that are based occupation of tetrahedral sites will be considered. Finally, (3)we will discuss some structures of mixed occupancy. Table 1.3 lists a number of representative compounds for each crystal structure type.

The most important example, perhaps, of an HCP-based oxide with octahedral site filling is corundum, the structure of the widely used ceramic, aluminum oxide(Al_2O_3). It is based on the HCP stacking of oxygen with 2/3 of the octahedral sites filled. We will examine this and some closely related derivative structures: $LiNbO_3$ and $FeTiO_3$. Derivative structures are more complex structures that can be derived, and are most easily understood, using a simpler structure. A tetrahedrally filled HCP structure of importance is wurtzite, in which one half of the tetrahedral sites are filled. (ZnO is one example.) A final HCP-based structure we will examine is rutile, the mineral name of the compound TiO_2, in which one half of the octahedral sites are also filled, but in such a way that the resulting symmetry of the crystal is actually tetragonal.

Ceramic Crystal Structures

- Those based on FCC anion close-packing

(1) The cations occupying octahedral sites.

(2) Occupation of tetrahedral sites.

(3) Some structures of mixed occupancy.

- Those based on HCP anion close-packing

(1) Only fraction of octahedral site filled: corundum.

(2) Some closely related with corundum derivative structures: $LiNbO_3$ and $FeTiO_3$.

(3) One half of the tetrahedral sites filled: wurtzite.

(4) One half of the octahedral sites filled: rutile.

Ceramic Crystal Structures

Table 1.3 Some Ceramic Crystal Structures

Structure	Stoichiometry	Anion Packing	Coordination Number around M and X	Examples	Derivative Structures
Rocksalt	MX	FCC	6, 6	NaCl, KCl, LiF, KBr MgO, CaO, SrO, BaO NiO, CoO, MnO, FeO, TiN, ZrN	
Zincblende	MX	FCC	4, 4	ZnS, BeO, SiC (3C), BN,GaAs, CdS, InSb	Diamond cubic (Si, Ge, C)
Wurtzite	MX	HCP	4, 4	ZnO, ZnS, AlN, SiC (2H)	
Nickel arsenide	MX	HCP	6, 6	NiAs, FeS, FeSe, CoSe	
Anti-fluorite	M_2X	FCC	4, 8	Li_2O, Na_2O, K_2O Rb_2O	
Fluorite	MX_2	Primitive cubic	8, 4	CaF_2, ZrO_2, UO_2, ThO_2, CeO_2	Pyrochlore ($A_2B_2O_7$), e.g., $Pb_2Ru_2O_7$, $Gd_2Ti_2O_7$, $Gd_2Zr_2O_7$ Bixbyite (e.g. Y_2O_3)
Cesium Chloride	MX	Primitive cubic	8, 8	CsCl, CsBr, CsI	
Rutile	MX_2	Distorted HCP	6, 3	TiO_2, SnO_2, GeO_2 MnO_2, VO_2, NbO_2 RuO_2, PbO_2, PbO_2	Defective "Magneli phases" of formula Ti_nO_{2n-1}

Ceramic Crystal Structures

Table 1.3 *continued*

Corundum	M_2X_3	HCP	6, 4	Al_2O_3, Cr_2O_3	Ilmenite ($FeTiO_3$) Lithium Niobate ($LiNbO_3$, $LiTaO_3$)
Perovskite	ABX_3	AO sublattice forms FCC	12, 6, 6	$CaTiO_3$, $SrTiO_3$ $BaTiO_3$, $PbTiO_3$ $LaGaO_3$, $LaAlO_3$ $BaZrO_3$, $PbZrO_3$ $Ba(Pb_{1-x}Bi_x)O_3$, $Ba_{1-x}K_xO_3$ $Pb(Zr, Ti)O_3$ $(Pb, La)(Zr, Ti)O_3$	Ordered solid solutions, e.g., $Pb(Mg_{1/3}Nb_{2/3})O_3$, $Pb(Sc_{1/2}Ta_{1/2})O_3$
Spinel	AB_2X_4	FCC	4, 6, 4	$MgAl_2O_4$, $FeAl_2O_4$ $ZnAl_2O_4$, $ZnFe_2O_4$ $MnFe_2O_4$, $LiTi_2O_4$	Many solid solutions are possible.
Inverse spinel	$B(AB)X_4$	FCC	4, 6, 4	Fe_3O_4, $CoFe_2O_4$ $NiFe_2O_4$, $MgFe_2O_4$	Many solid solutions.
"K_2NiF_4"	A_2BX_4	Alternating perovskite and rocksalt type layers	9, 6, 6	K_2NiF_4, La_2CuO_4 $La_{2-x}Sr_xCuO_4$, La_2NiO_4	"Ruddlesden-Popper" phases $AO{\cdot}nABO_3$, e.g., Sr_2TiO_4, $Sr_3Ti_2O_7$; high temperature oxide superconductors of formula $mAO{\cdot}nABO_3$ such as $Bi_2Sr_2CaCu_2O_8$, $Tl_2Ba_2Ca_2Cu_3O_{10}$.

Ceramic Crystal Structures

Table 1.3 *continued*

"$YBa_2Cu_3O_7$"	$AB_2C_3X_7$	Perovskite-like with missing oxygens	8, 10, 5 or 4, 6	$YBa_2Cu_3O_7$, $MBa_2Cu_3O_7$, where M = Eu, Dy, Ho, Er, Yb	$Y_2Ba_4Cu_7O_x$, $Y_2Ba_4Cu_8O_x$
Silicates (quartz, tridymite crystobalite)	AX_2	Corner-shared SiO_4 tetrahedra	4, 2	SiO_2, GeO_2	β-eucryptite ($LiAlSiO_4$) is a quartz derivative; many other crystalline silicates of similar coordination; network glasses.
Silicon nitride	A_3X_4	Corner shared SiN_4 tetrahedra	4, 3	α- Si_3N_4, β-Si_3N_4	Silicon oxynitrides solid solutions (sialons) with valence-compensating cation and anion substitutions.

Ceramic crystal structures

- **FCC-based Structures**

Rocksalt.

Anion lattice: FCC
Cation filling: all octahedral sites
The r_C/r_A : 0.414~0.732
Stoichiometry: MX
Example :NaCl, KCl, LiF, MgO, CaO, SrO, NiO, CoO, MnO, PbO, et al.

For NaCl the bond strength contributed by a cation is 1/6. The coordination number of anions around cations is the same as that of cations around anions: six. Therefore the sum of bond strengths reaching a chlorine ion is the valence of the chlorine ion (6(1/6)=1) as predicted by the second rule.

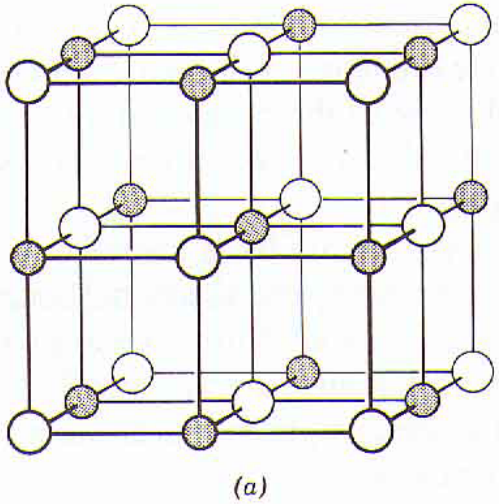

(a)

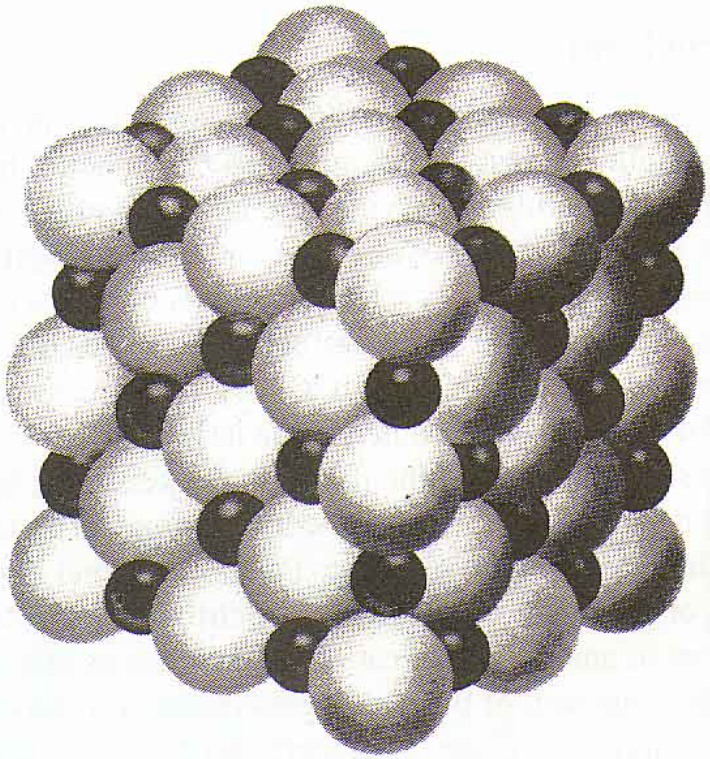

(b)

Fig. 1.13 Crystal structure of sodium chloride.

Ceramic crystal structures

- **FCC-based Structures**

Antifluorite.

Anion lattice: FCC

Cation filling: all tetrahedral sites

Coordination number:

X 8; M 4

Stoichiometry: M_2X

Example :Na_2O, Li_2O, K_2O,

Figure on the right shows one unit cell of the structure compound Li_2O.

The Li ions are somewhat larger than we would expect in tetrahedral sites, but there are too many for the available octahedral sites, so occupying the tetrahedral sites is the next best thing.

The bond strength is ¼, so, CN of O should be eight according to the second rule.(8×1/4=2)

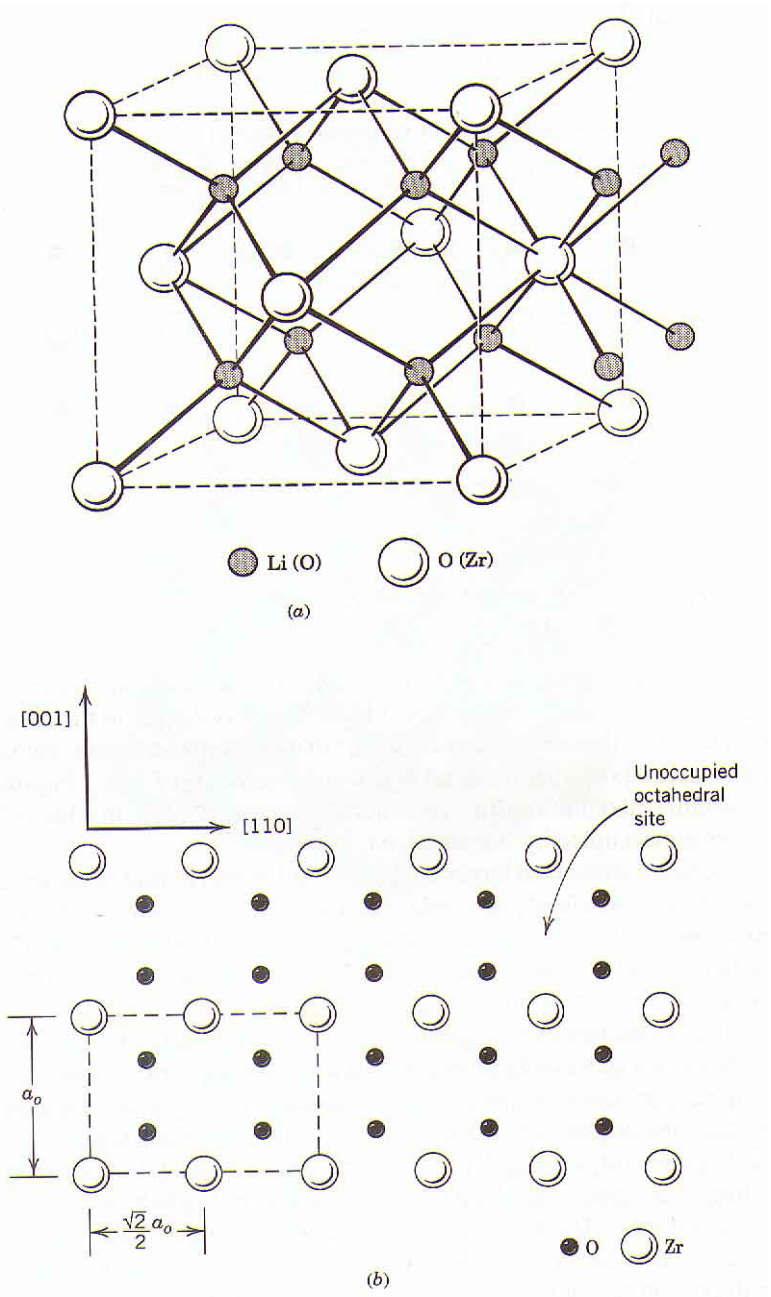

Fig. 1.15 (*a*) Antifluorite (fluorite) structure, typified by compounds Li_2O and ZrO_2. (*b*) (110) plane of the fluorite structure compound ZrO_2.

Ceramic crystal structures

- **FCC-based Structures**

Fluorite.

Cation lattice: FCC **Anion filling: all tetrahedral sites**

Stoichiometry: MX_2 **Coordination number: X 4; M 8**

Example :CaF_2, ZrO_2, UO_2, CeO_2.

We can envision it simply by reversing the cation and anion position in the antifluorite structure.

Note also that there exists a large unoccupied octahedral site in the body-center and along each edge of fluorite unit cell. UO_2 (uranium oxide) is a useful basis for nuclear fuels in part because this large interstice is able to accommodate various fission products.

Cubic bixbyite: the structure in which Y_2O_3 crystallizes

Pyrochlore: the structure, such as $Pb_2Ru_2O_7$, $Gd_2Ti_2O_7$, $Gd_2Zr_2O_7$,

derivatives of fluorite structure; oxygen deficient with respect to the stoichiometry of fluorite; one out of every four or one out of every eight oxygen are missing; ordered arrangement of oxygen vacancies leads to a cubic unit cell composed of eight fluorite type cells.

The intrinsically high concentration of oxygen vacancies→good oxygen ion conduction →oxygen sensor materials

Ceramic crystal structures

- **FCC-based Structures**

Zincblende.

Anion lattice: FCC
Cation filling: half of tetrahedral sites
Stoichiometry: MX
Example :ZnO, ZnS, BeO.
SiC, BN, GaAs

Smaller cation;
Tetrahedral sites in FCC form a primitive cubic array,
and half of them on the opposing corners of the cube are filled, in order to achieve maximum cation separation.
Many covalence compounds in the structure, but for quite different reason. Covalence bond results from the overlap of sp^3 hybridized orbitals with tetragonal directionlality.

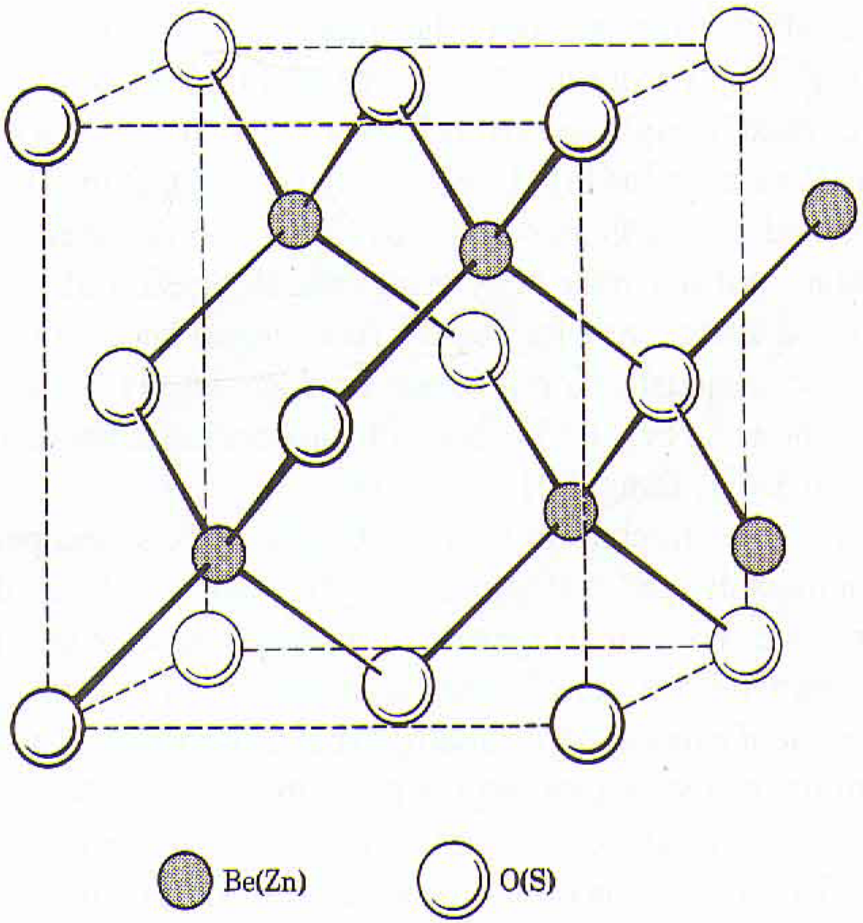

Fig. 1.16 Zincblende (ZnS) structure.

Ceramic crystal structures

- **HCP-based Structures**

Wurtzite.

Anion lattice: HCP
Cation filling: half of tetrahedral sites
Stoichiometry: MX
Example :ZnO, ZnS, AlN, SiC(2H)
Coordination: 4,4
Madelung constant α: 1.641

The wurtzite also meets the requirements of Pauling's second rule.
The Madelung constants of zincblende and wurtzite structures are very similar(1.638 and 1.641). Since each has one-half of tetrahedral sites filled as well it is reasonable that the compounds often have a polytype. Furthermore, it is the preferred structure of a number of covalent compounds, including AlN and the α phases of SiC.

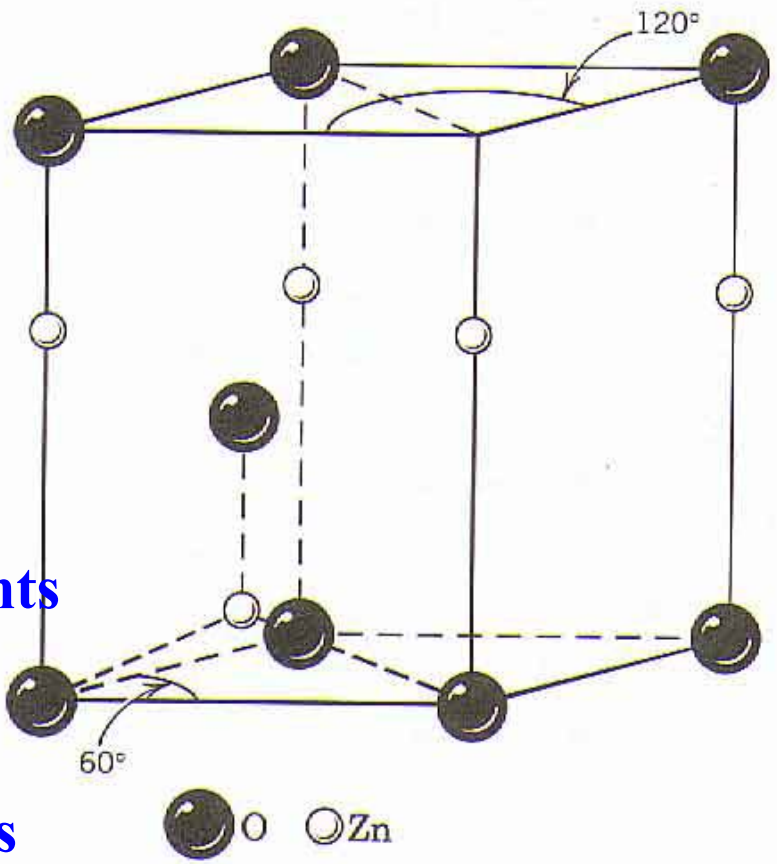

Fig. 1.18 Unit cell of the wurtzite structure.

Ceramic crystal st

- **HCP-based Structures**

Corundum.

Anion lattice: HCP

Cation filling: two-thirds of octahedral sites

Stoichiometry: M_2X_3, MMX_3

Example : Al_2O_3, Cr_2O_3, Fe_2O_3

Coordination: 6, 4

Madelung constant α: 4.040

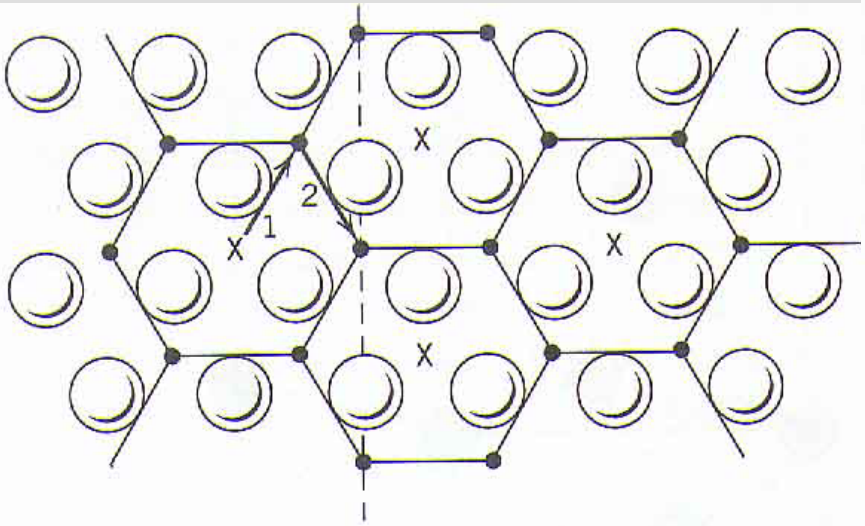

Fig. 1.19 Filling of 2/3 of the octahedral sites in the basal plane of corundum. Only one close-packed anion plane is shown.

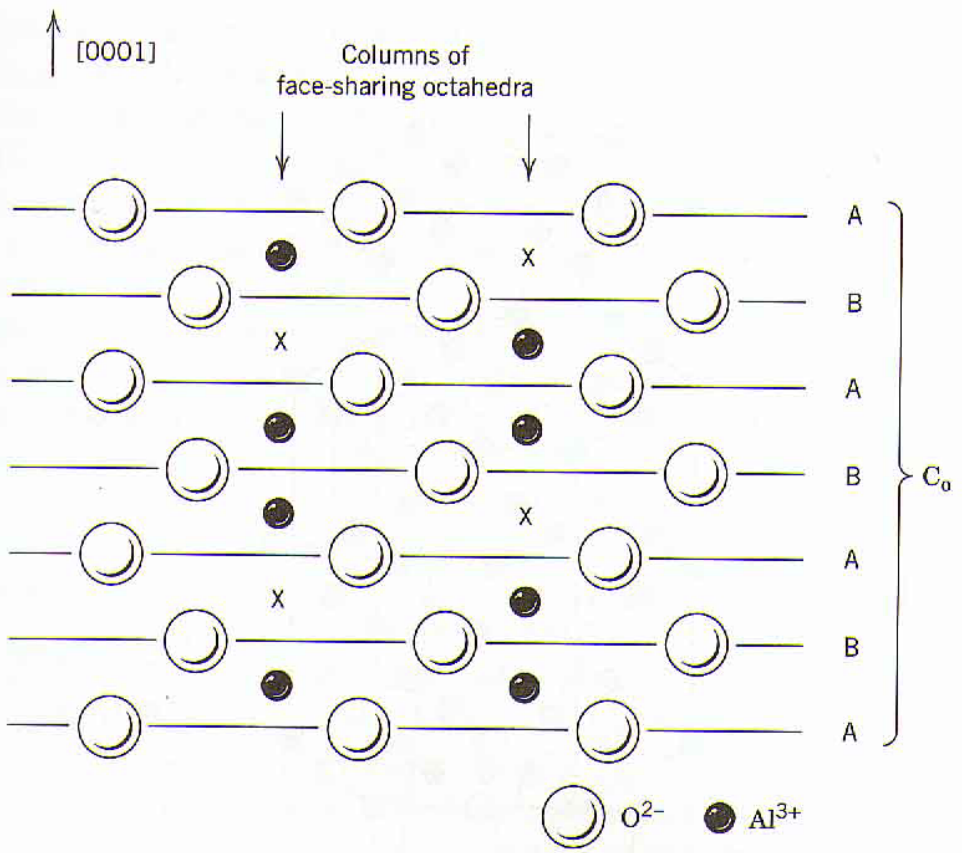

Fig. 1.20 Plane shown by dashed line in Fig. 1.19. Two-thirds occupancy of the columns of octahedral sites is shown.

From Fig.1.20, the cation sublattice repeats after three layers, anion sublattice repeats after two layers, so the structure repeats itself after six layers, giving rise to 12.99 angstrom c_0 unit cell dimension.

Ceramic crystal structures

- **HCP-based Structures**

Ilmenite and Lithium Niabate.

Anion lattice: HCP
Cation filling: two-thirds of octahedral sites
Stoichiometry: MMX_3
Example : $FeTiO_3$, $LiNbO_3$
Coordination: 6, (2,2)

Ilmenite

As on corundum, two-thirds of the octahedral sites are filled, in the case by an ordered substitution of Fe and Ti for Al. The arrangement shown in Fig.1.20 is preserved, but with alternating cation layers occupied by Fe and Ti alone.

Six layer sequence is required to repeat the structure.

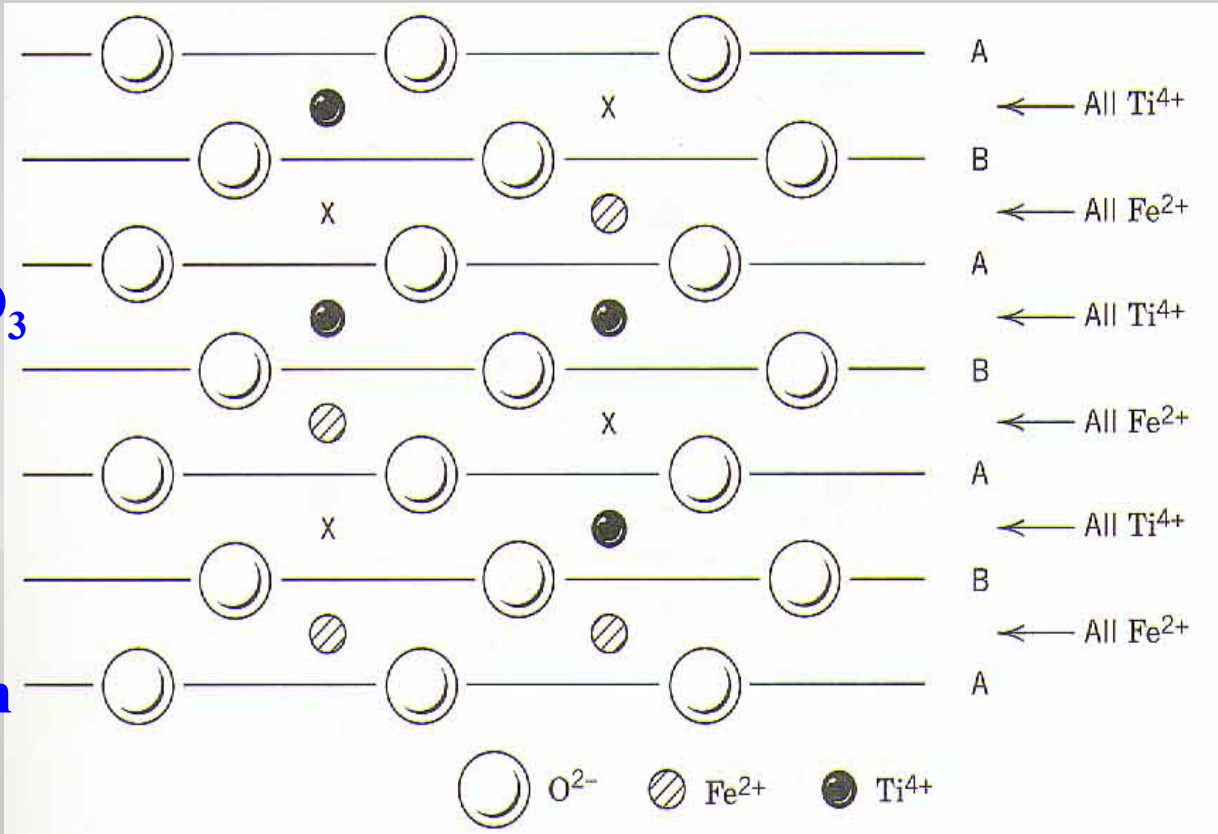

Fig. 1.22 Ilmenite structure in same projection as Fig. 1.20.

Ceramic crystal structures

- **HCP-based Structures**

Lithium Niobate

Notice that each of the Li-Nb pairs in Fig.1.24(cross-section) is oriented in the same direction. Due to the charge distribution between the Li-Nb pair, a net electric dipole exists for each of the pairs in the structure.
Anisotropy →Birefringence !!

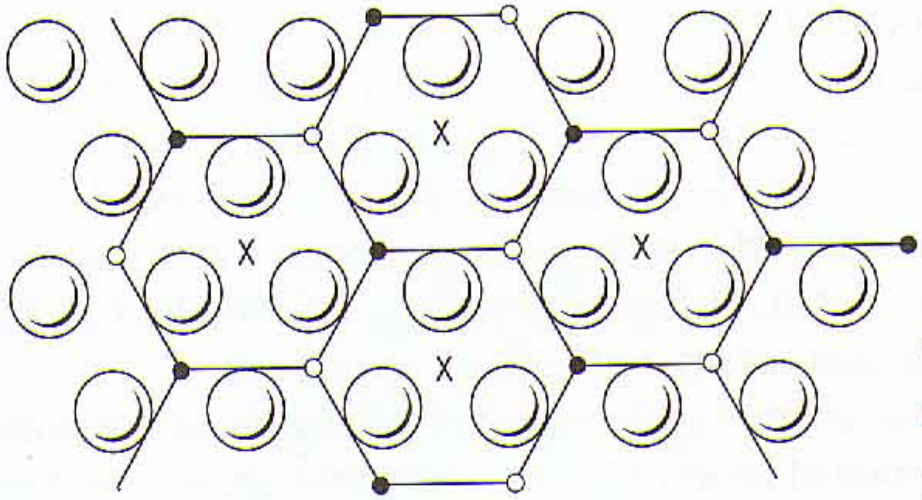

Fig. 1.23 Basal plane of $LiNbO_3$ structure, showing mixed Li, Nb occupancy.

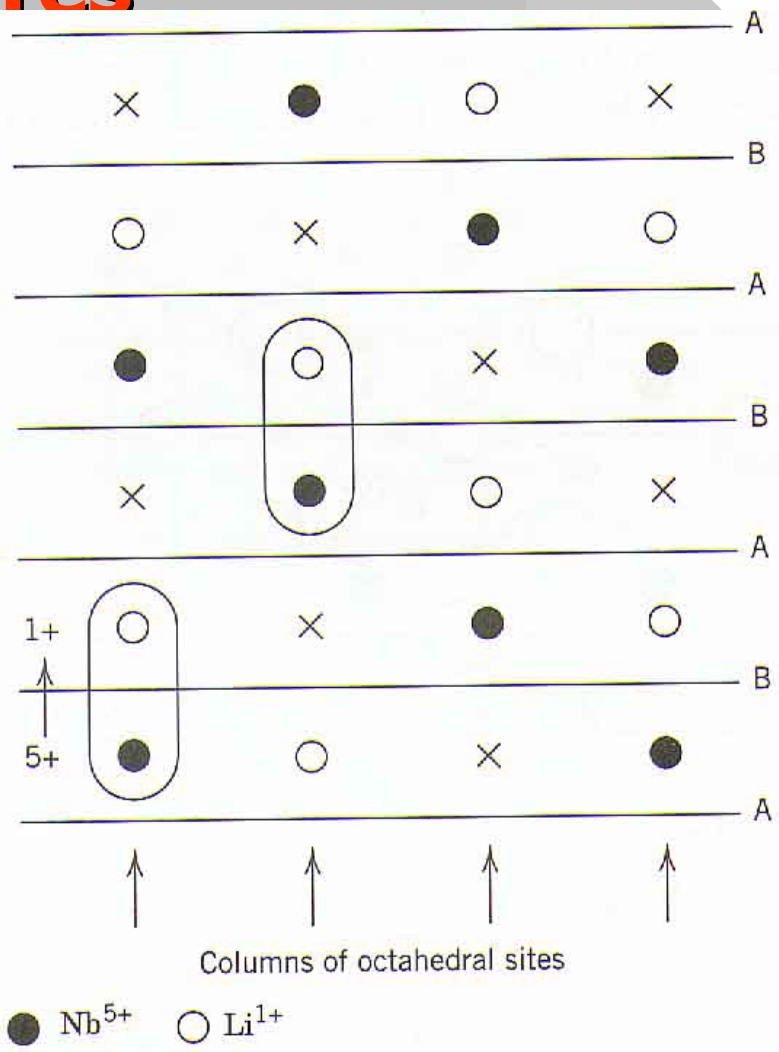

Fig. 1.24 Cation arrangement in $LiNbO_3$, showing orientation of dipole between Li^{1+} and Nb^{5+}.

Ceramic crystal structure

- **HCP-based Structures**

Rutile.

Anion lattice: HCP
Cation filling: half of octahedral sites
Stoichiometry: MX_2
Example : TiO_2, SnO_2, MnO_2
Crystal structure: tetragonal

Column empty octahedral site→ anisotropy →anisotropic diffusion anisotropic refractive index.

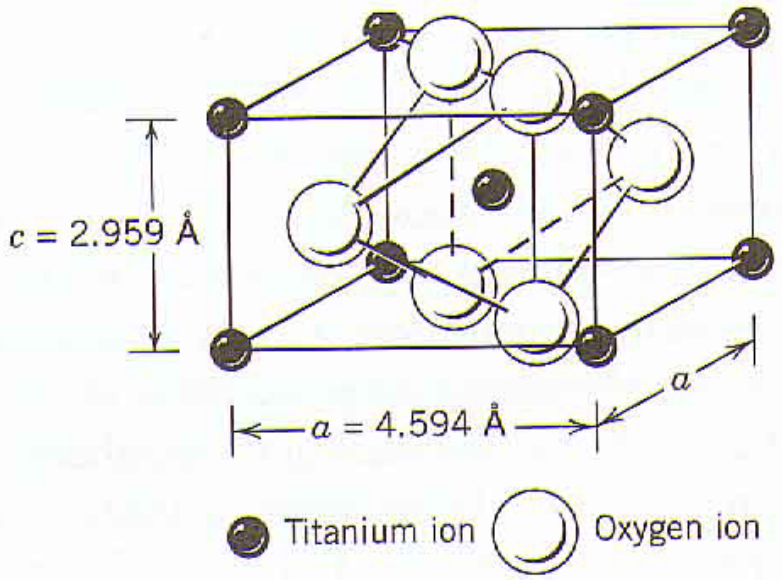

Fig. 1.26 Unit cell of rutile structure.

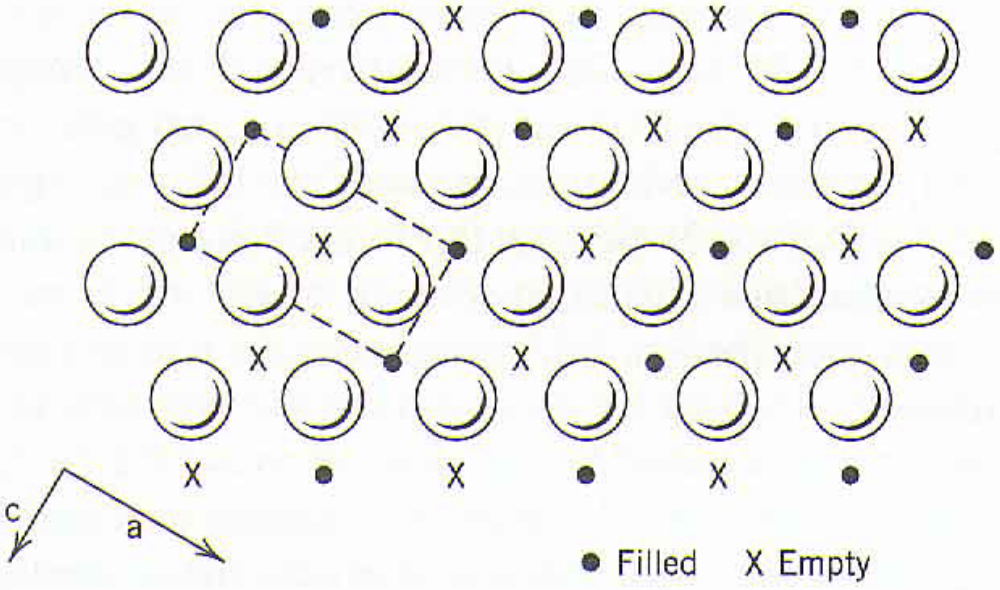

Fig. 1.25 One-half filling of octahedral sites in a close-packed plane (rutile structure).

Ceramic crystal structures

Perovskite.

Stoichiometry: ABX_3, and A and B cations differ considerable in size.
FCC-derivative structure; Large A cation and oxygen lattice: FCC
Small cation filling: octahedral sites, only oxygen as its nearest neighbors
Example : $BaTiO_3$, $CaTiO_3$, $PbZrO_3$, $LaAlO_3$
Crystal structure: cubic

Notice that the Ti and Ba Ions are shielded from one another be oxygen.

The bond strength of Ba and Ti are 2/12 and 4/6, Each oxygen ion is co-ordinated by four Ba and two Ti ions. So $4\times(2/12)+2(4/6)=2$ Pauling's second rule is satisfied.

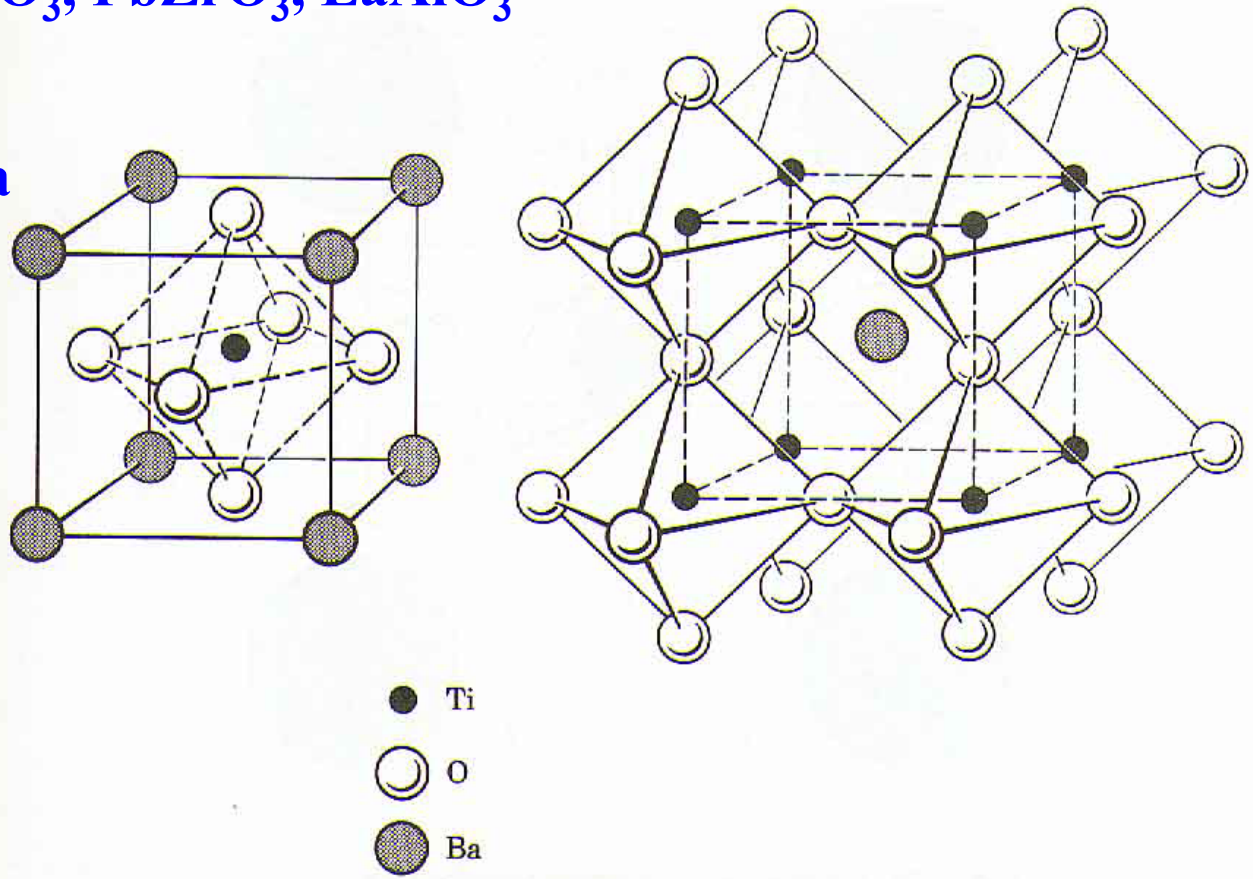

Fig. 1.27 Ion positions in ideal cubic perovskite structure.

Ceramic crystal structures

Spinel.

Stoichiometry: AB_2O_4, ($AO \cdot B_2O_3$).
Anion lattice: FCC
Cation filling: one-eighth of tetrahedral sites and one-half octahedral sites
Example : $MgAl_2O_4$,
Crystal structure: cubic

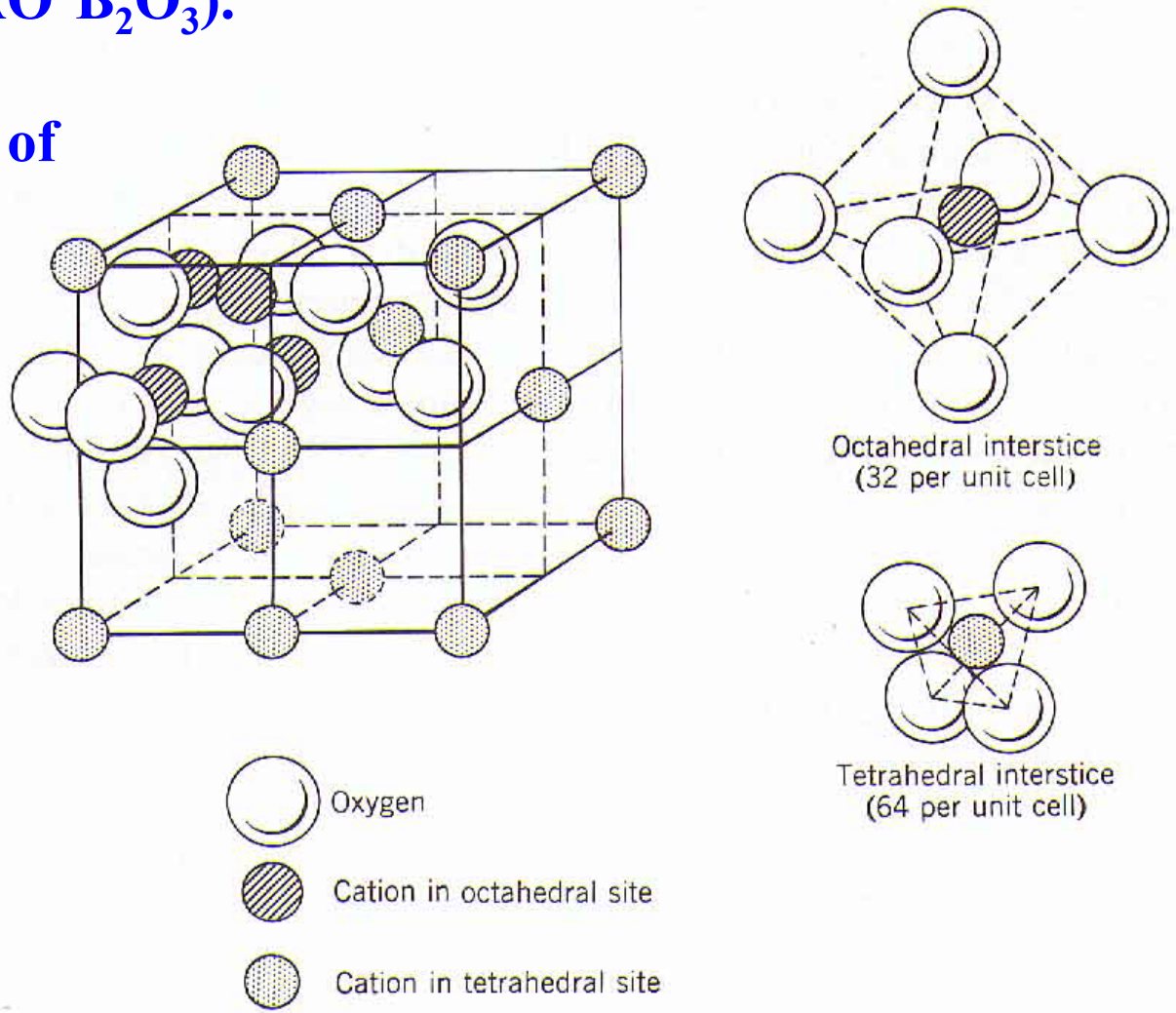

Fig. 1.30 Atomic layers parallel to the (001) plane in spinel.

Defects in Ceramics

Introduction.

We have primarily discussed the ideal crystalline state. However, a great many properties of crystals are determined by imperfects. Electrical conductivity and diffusional transport in most ceramics is determined by the number and type of defects. Various optical properties, for instance those giving rise to color and lasing activity, are caused by electronic absorption and emission processes at impurity ions and point defects. The rates of kinetic processes such as precipitation, densification, grain coarsening, and high-temperature creep deformation are determined by mass transport due to defects.

A principle difference between point defects in ionic solids and those in metals is that in the former, all such defects can be electrically charged.

Ionic defects are point defects that occupy lattice atomic positions, including vacancies, interstitials, and substitutional solutes.

Electronic defects are deviations from the ground state electron orbital configuration of a crystal, formed when valence electrons are excited into higher orbital energy levels. Such an excitation may create an electron in the conduction band and/or an electron hole in the valence band of the crystal.

Point Defects

Two principle issues: Type and Concentrations of defects.

Clues to defects:

Melting temperature.

Defects→breaking of bonds→strength of bonding→melting temperature →energy to form defects →homologous temperature T/T_m

The availability of defect sites.

For instance, in the rock salt structure, anion interstitial have a high energy relative to other defects such as anion vacancies, cation vacancies and cation interstitial.

The compatibility in size and valence between solutes(impurities) and host.

It is necessary to consider the energy to form the charge-compensating defect.

Chemical composition.

In nonstoichiometric compounds, defects density often is high due to the existence of multiple ion valence states. For example, wustite ($Fe_{1-x}O$).

Electrical conductivity.

directly related to the concentration of mobile electronic defects, low conductivity →low electron or hole concentration, …

Point Defects

1. Intrinsic Ionic Disorder

Atomic defects are formed with expenditure of energy which is most commonly thermal, although radiation of various kinds can also displace atoms.

Two most common types of crystalline defects in ionic materials:
Frenkel and Schottky defects

Frenkel pair:
In ionic materials, both the cation and the anion can undergo this kind of displacement. In metals and covalent compounds Frenkel defects can also form; they differ from those in ionic compounds only in that the defects need not be electrically charged.

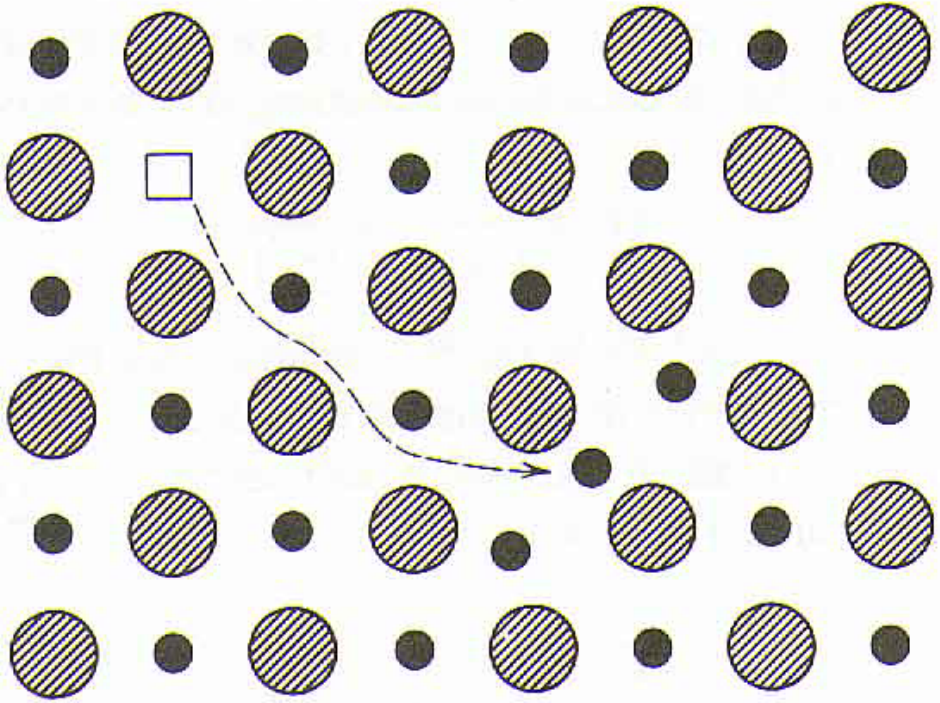

Fig. 2.1 Frenkel disorder. Ion leaving normal site forms an interstitial ion and leaves a vacancy.

Point Defects

1. Intrinsic Ionic Disorder

Schottky defects:

The vacancy must be formed in the stoichiometric ratio in order to preserve the electrical neutrality of the crystal. Thus in NaCl and MgO, One forms a Schottky pair, while in TiO_2 the the Schottky defect consists of three defects (one titanium vacancy and two oxygen vacancies), and in Al_2O_3, the Schottky defect is a quintuplet. The total number of lattice sites is increased by one formula unit upon formation of Schottky defect, unlike the the Flenkel defect, which conserves the number of lattice sites.

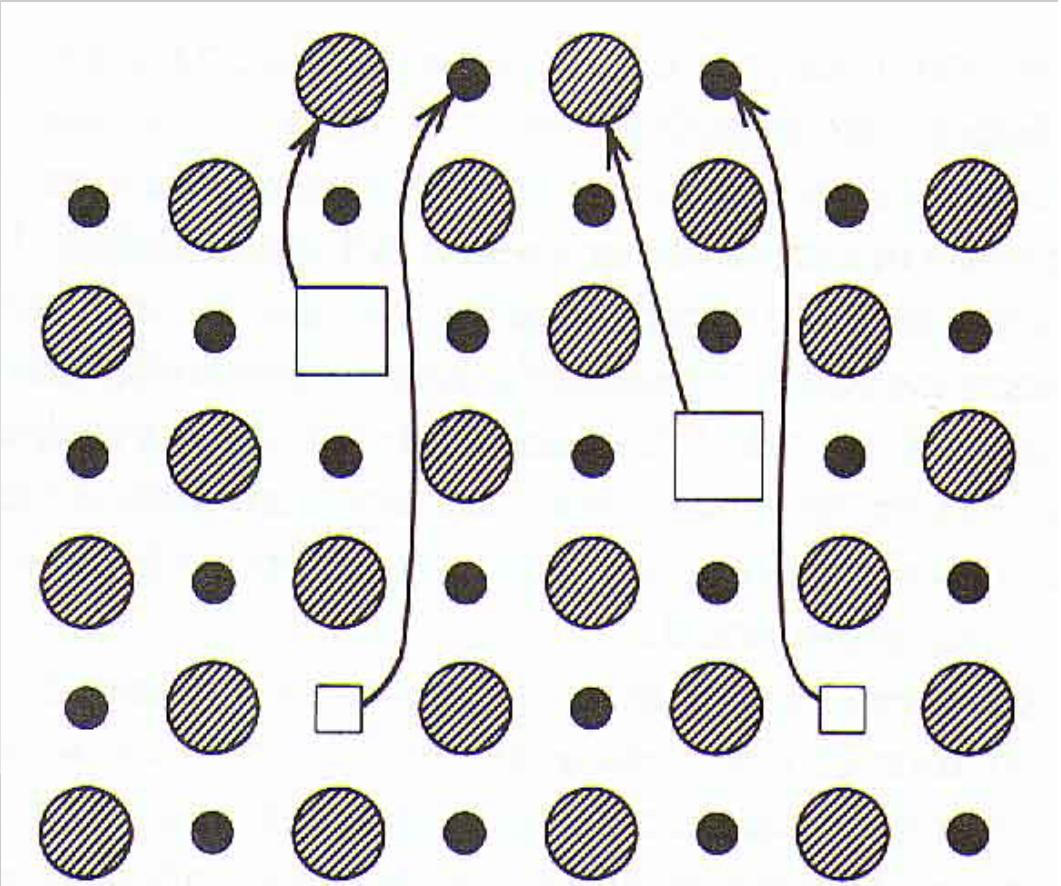

Fig. 2.2 Schottky disorder. Displacement of anion and cation to surface leaves a pair of vacancies.

Point Defects

2. Concentration of Intrinsic Defects

The concentration of defects is given as the fraction of the total number of atoms N as following:

$$\frac{n}{N} = \exp\left[-\frac{\Delta g}{2kT}\right] = \exp\left[\frac{\Delta s}{2k}\right]\exp\left[-\frac{\Delta h}{2kT}\right] \approx \exp\left(-\frac{\Delta h}{2kT}\right)$$

Table 2.1 Defect Concentration at Different Temperatures

Defect Concentration	1eV[a]	2eV	4eV	6eV	8eV
n/N at 100°C	2×10^{-7}	3×10^{-14}	1×10^{-27}	3×10^{-41}	1×10^{-54}
n/N at 500°C	6×10^{-4}	3×10^{-7}	1×10^{-13}	3×10^{-20}	8×10^{-27}
n/N at 800°C	4×10^{-3}	2×10^{-5}	4×10^{-10}	8×10^{-15}	2×10^{-19}
n/N at 1000°C	1×10^{-2}	1×10^{-4}	1×10^{-8}	1×10^{-12}	1×10^{-16}
n/N at 1200°C	2×10^{-2}	4×10^{-4}	1×10^{-7}	5×10^{-11}	2×10^{-19}
n/N at 1500°C	4×10^{-2}	1×10^{-4}	2×10^{-6}	3×10^{-9}	4×10^{-12}
n/N at 1800°C	6×10^{-2}	4×10^{-3}	1×10^{-5}	5×10^{-8}	2×10^{-10}
n/N at 2000°C	8×10^{-2}	6×10^{-3}	4×10^{-5}	2×10^{-7}	1×10^{-9}

Here N is the number of atoms, n the number of the defects, Δg the formation free energy. Note that the entropy Δs is not the configuration entropy, which is the nonconfiguration entropy associate with lattice strains and changes in vibrational frequencies accompanying the defect. Since the values of exp(Δs/2k) range from 10^{-4} to 10^{4}, the absolute concentrations of intrinsic defects can be difficult to determine to a high level of accuracy.

Point Defects

3. Intrinsic versus Extrinsic Behavior

The concentration of intrinsic defects can be exceedingly small in highly refractory ceramics of large defect formation energy. As a result, solutes and especially aliovalent solutes which are accompanied by the formation of extrinsic vacancies or interstitials have a great importance in determining overall defect behavior. Oxidation and reduction processes also cause point defects to be introduced, the concentrations of which can exceed that of the intrinsic ionic defects. Intrinsic defect concentrations increase with temperature, as discussed above. Extrinsic defects, with the exception of nonchiometry, remain largely constant in concentration. Thus at higher temperatures, the likelihood of intrisic behavior increases. However, in some materials the formation energies of intrinsic defects are so high, and the resulting concentrations so low, that intrinsic behavior is virtually never encountered.

As an example, let us consider the relative importance of intrinsic defects in two compounds of rocksalt structure type, NaCl and MgO. In both, the dominant intrinsic defect is the Schottky defect, as opposed to cation or anion Frenkel defects. For charge neutrality the concentration of cation and anion vacncies must be equal.

Point Defects

3. Intrinsic versus Extrinsic Behavior

From the Eq. in the transparency before last, we can write the concentration of each vacancy as

$$n_v / N \sim \exp\left[-\Delta h_s / 2kT\right]$$

The Schottky formation enthalpy for MgO (~7.7 eV) is much higher than that for NaCl (~2.4 eV), consistent with the stronger bonding and higher melting temperature (2825 ˚C vs 801 ˚C) of former. At 700 ˚C, MgO clearly has many orders of magnitude fewer intrinsic Schottky defects. Scaled to the homologous temperature, the concentrations are not so different; at melting point NaCl has a defect concentration of ~2×10^{-6} (2 parts per million, ppm) and MgO has ~4×10^{-7} (0.4 ppm).

However, there is a great difference in the purity levels attainable in these two materials. With zone-refining procedures, NaCl can be purified to levels below one part-per-million. In contrast, the highest purity MgO currently available has about 50 ppm impurities (because of the much higher processing temperatures necessary, contamination from crucibles and the like is harder to avoid). These impurities are often aliovalent cations. Thus the concentration of "extrinsic"defect is much greater than the intrinsic defect's in MgO. As a result, "intrinsic" NaCl can be achieved rather easily, whereas all presently available MgO is likely to be extrinsic at all temperatures up to the melting point.

Point Defects

4. Units for Defect Concentration

A variety of units are used in the description of defect concentration.

The two most common systems of units are the number fraction relative to particular atom(atomic fraction, cation fraction, or mole fraction, which are usually used in materials science), and the number of defects per unit volume(usually using in physics).

Note that trace chemical analyses are often reported in units of weight ppm or weight percent instead.

An exact conversion from mole fraction to number per unit volume requires knowing the molecular weight(*MW*) and desity(ρ) of the compound in question; the number of formula units per unit volume is

$$\frac{N_a(no./mole)\cdot\rho(g/cm^3)}{MW(g/mole)}$$

Where N_a is Avogadro's number (6.02×10^{23}).

The density of atoms in solids is ~10^{23} cm^{-3}, so a 1 ppm concentration is ~10^{17} cm^{-3}.

Point Defects

5. Kröger-Vink Notation

A standard notation used in ceramics for the description of defects in ionic materials is *Kröger-Vink* notation, in which a defect is described by three parts.

1. The main body of the notation identifies whether the defect is a vacancy "V", or an ion such as "Mg".
2. The subscript denotes the site that the defect occupies, either the normal atom sites of the host lattice or an interstitial site "i".
3. The superscript identifies the effective charge (or relative charge) of the defect relative to the perfect crystal lattice. For this part of notation, dots ($^{\cdot}$) represent positive effective charges, dashes ($'$) represent negative charge, and x's are sometimes used to show neutrality.

Now let's illustrate with some examples: V''_{Mg} is a vacant magnesium site; V stands for vacancy, the subsctipt Mg shows that it occupies what is normally a magnesium site, and, the superscript $''$ shows that the vacancy has a doubly negative charge relative to the perfect lattice, as there is the absence of an Mg^{2+} ion.

$Al_i^{\cdot\cdot\cdot}$ is an interstitial aluminum ion. The subscript i denotes that the aluminum site, and, the superscript $^{\cdot\cdot\cdot}$ shows that the normally unoccupied interstitial site now has an excess +3 charge due to the Al^{3+} ion.

Point Defects

5. Kröger-Vink Notation

The concentration of defects is denoted by square brackets, for example $\left[V''_{Mg}\right]$, $\left[Al^{\bullet}_{Mg}\right]$ and $\left[\left(V'_{Na} - V^{\bullet}_{Cl}\right)^{x}\right]$. A shorthand often used for the concentration of electrons and holes, [e´] and [h˙], is *n* and *p*, respectively.

Finally, in Kröger-Vink notation we always define defects relative to a "perfect" crystal. For complex ceramics with multiple cations distributed over more than one type of site, such as the spinels (which can have a normal, reverse, or random cation distribution), the choice of this reference state can be somewhat arbitrary. Nonetheless, defect chemical notation and the principles discussed herein can be applied as long as the reference system is self-consistent throughout.